Highly active and selective supported iron oxide nanoparticles in microwave-assisted *N*-alkylations of amines with alcohols

Camino Gonzalez-Arellano,[a] Kenta Yoshida,[b] Rafael Luque*[c] and Pratibha L. Gai[b,d]

Received 19th February 2010, Accepted 25th March 2010
First published as an Advance Article on the web 18th May 2010
DOI: 10.1039/c003410j

Highly active and stable supported iron oxide nanoparticles show excellent activities and switchable selectivities to target products in the microwave-assisted *N*-alkylation of amines with alcohols.

N-Alkylation reactions through hydrogen autotransfer processes are very attractive strategies in organic synthesis,[1,2] granting access to a wide variety of important chemicals that find applications as dyes, pharmaceuticals, agrochemicals, surfactants and biologically active compounds.[3] These approaches have also significant advantages compared to conventional alkylations and hydroaminations including the simplicity of the protocol, availability of starting materials and most importantly the variety of catalysts able to carry out these reactions.

With regards to the catalysts employed in hydrogen autotransfer processes, the majority are homogeneous catalysts in which transition metal complexes and salts including Ru, Ir, Rh, Pt and Au have been extensively reported.[1,2,4] Transition metal-free protocols have also been reported, although they normally require harsh reaction conditions (high temperatures and pressures) to achieve reasonable yields of products.[1,5]

Compared to homogeneous catalysts, heterogeneously catalysed methodologies based on silicon and aluminium,[6] Ni,[7] Cu,[8] Pt[9] and more recently an unmodified commercial magnetite[10] have been proposed as alternatives. However, all reported protocols are generally energy intensive (taking 24 h + to complete),[1,6,10] with catalysts having poor recyclabilities and employ salts and/or catalysts that cannot be properly reused upon reaction completion. Furthermore, these approaches are also limited as the methodologies normally work only with activated compounds (*e.g.* aromatics), being completely ineffective for less activated systems (*e.g.* alkyl derivatives).

In our recent studies towards more environmentally friendly catalysts and benign reaction conditions, we have reported the preparation of highly active, selective and reusable supported iron and iron oxide nanoparticles on a variety of porous materials in the oxidation of alcohols.[11] Among the reported catalysts, Fe-MCM-41 was found to be highly active and reusable in the reaction, preserving its initial activity after 5 uses.[11] These catalysts were proved to be environmentally compatible and cheaper alternative catalysts for a wide range of reactions[11,12] that are especially valuable to the pharmaceutical industry.

Following these preliminary studies in the development of highly active and reusable supported Fe materials, we report here, for the first time, the activity of supported Fe oxide nanoparticles in the microwave assisted selective *N*-alkylation between anilines and benzyl alcohols mediated by hydrogen autotransfer (Scheme 1).

Scheme 1 *N*-Alkylation of aniline with benzyl alcohol.

Experimental

Materials preparation

Materials were synthesized following a similar protocol to that previously reported our group,[11] using $FeCl_2{\cdot}4H_2O$ as Fe precursor and ethanol–water as solvent under microwave irradiation.

A typical preparation of the iron supported catalysts was performed as follows: 0.2 g support were suspended in 2 mL EtOH containing 100 mg $FeCl_2{\cdot}4H_2O$ and microwaved at 200 W for 15 min (average temperature 100 °C, 120 °C maximum temperature reached). Solids were then filtered off, washed with an excess of ethanol and acetone and dried overnight at 100 °C. The red-orangish powders (supported Fe oxide nanoparticles) were characterised by means of several techniques including Nitrogen physisorption, Aberration Corrected (Scanning)-high angle annular dark field Transmission Electron Microscopy (AC-HAADF-TEM/STEM), X-Ray Diffraction (XRD) and X-Ray Photoelectron Spectroscopy (XPS).

Different supports were chosen to investigate the effect of the stabilisation of the nanoparticles on the properties and activity of the materials in the alkylation. These include porous (silica, MCM-41 and a mild acidic montmorillonite clay) and non porous biomaterials (cellulose and chitosan).

Si-MCM-41 and hexagonal mesoporous silica (HMS) were prepared according to previously reported protocols from our

[a]*Green Chemistry Centre of Excellence, University of York, York, UK*
[b]*Nanocentre, Chemistry Department, Heslington, YO10 5DD, York, UK*
[c]*Dpto. Química Orgánica, Universidad de Córdoba, Campus de Rabanales, Edif..Marie Curie, Ctra Nnal IV, Km 396, E14014, Córdoba, (Spain). E-mail: q62alsor@uco.es; Fax: +34 957212066; Tel: +34957212065*
[d]*Department of Physics, University of York, YO10 5BR, York, UK*

group.[13,14] Commercial montmorillonite KSF clay (Fluka), cellulose (Sigma, cellulose fibrous medium) and chitosan (Aldrich, medium molecular weight, 75-85% deacetylated) were used as purchased.

Materials characterisation

Nitrogen adsorption measurements were carried out at 77 K using an ASAP 2010 volumetric adsorption analyzer from Micromeritics. The samples were outgassed for 2 h at 100 °C under vacuum ($p < 10^{-2}$ Pa) and subsequently analyzed. The linear part of the BET equation (relative pressure between 0.05 and 0.22) was used for the determination of the specific surface area. The pore size distribution was calculated from the adsorption branch of the N_2 physisorption isotherms and the Barret-Joyner-Halenda (BJH) formula. The cumulative mesopore volume VBJH was obtained from the PSD curve.

The electron microscopy images were recorded in a JEOL 2200FS with double aberration correction (AC-TEM/STEM and HAADF-STEM), with integral in-column energy filter, operating at 200 kV and at the highest atomic scale resolution (0.1 nm or below) with crystallographic and chemical analysis. The dual aberration-correctors allow AC-TEM and AC-STEM imaging from the same regions of the nanocatalyst sample, providing powerful insights into the catalyst nanostructure. Aberration corrected high-angle annular dark-field TEM (AC-HAADF-TEM) were also recorded to directly image the isolated metal centres. Due to its sensitivity to atomic number, HAADF can image heavy atoms that appear as bright spots in the experiments (Fig. 1 to 2).[15] With aberration correction, a continuous range of interpretable spatial frequencies can be transferred by the optics without the contrast inversions, therefore the data are much more directly interpretable. More directly interpretable (sub) Angstrom level imaging, complemented by compositional data, uniquely provides new direct insights into the structure of

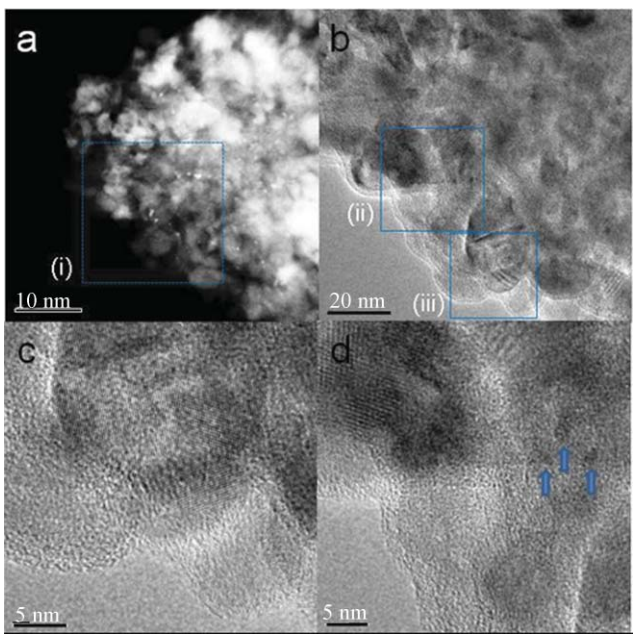

Fig. 1 a) AC-HAADF-STEM image; b) to d) AC-TEM images of Fe-Cellulose prepared by microwave deposition.

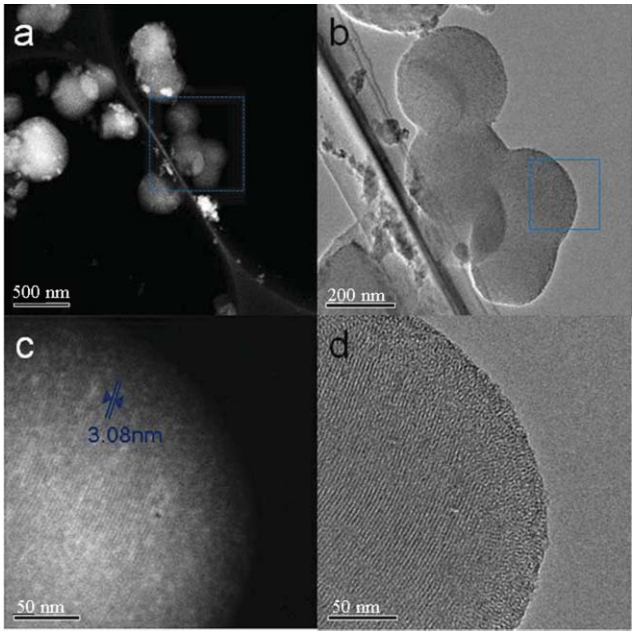

Fig. 2 a) AC-HAADF-STEM image; b) to d) AC-TEM images of Fe-HMS material prepared by microwave deposition.

nanoparticles, critical to understanding the nanostructures and reactivity properties of nanocatalysts. In high angle annular dark field STEM (HAADF-STEM) imaging we exploit the fact that electrons scattered at high angles (>30mrad) obey Rutherford's scattering law, with the scattering cross section proportional to Z2 where Z is the atomic number. A HAADF detector is used for imaging. Imaging of the highly scattered electrons using a HAADF STEM detector allows the detection of catalyst nanoparticles with higher Z, on lighter supports.

For AC-TEM/STEM studies, samples were prepared by ultrasonically dispersing as-synthesised catalyst powders in alcohol and placing the solution on holey carbon coated copper microgrids. Low dose electron beam imaging methods were employed throughout.

XPS measurements were performed in a ultra high vacuum (UHV) multipurpose surface analysis system (SpecsTM model, Germany) operating at pressures <10-10 mbar using a conventional X-Ray source (XR-50, Specs, Mg-Kα, 1253.6 eV) in a "stop-and-go" mode to reduce potential damage due to sample irradiation. The survey and detailed metal high-resolution spectra (pass energy 25 and 10 eV, step size 1 and 0.1 eV, respectively) were recorded at room temperature with a Phoibos 150-MCD energy analyser. Powdered samples were deposited on a sample holder using double-sided adhesive tape and subsequently evacuated under vacuum (<10-6 Torr) overnight. Eventually, the sample holder containing the degassed sample was transferred to the analysis chamber for XPS studies. Binding energies were referenced to the C1s line at 284.6 eV from adventitious carbon.

Metal content in the materials was determined using Inductively Coupled Plasma (ICP) in a Philips PU 70000 sequential spectrometer equipped with an Echelle monochromator (0.0075 nm resolution). Samples were digested in HNO_3 and subsequently analysed by ICP/AES at the University of Newcastle.

Catalytic tests

Alkylation reactions under microwave irradiation were carried out in a Microwave CEM-DISCOVER reactor with PC control and monitored by sampling aliquots of reaction mixture that were subsequently analysed by Gas Chromatography-Mass Spectrometry (GC/GC-MS) using an Agilent 6890 N GC model equipped with a 7683B series autosampler fitted with a DB-5 capillary column and an FID detector. Experiments were conducted in a closed vessel (pressure controlled) under continuous stirring. The microwave method was generally power controlled. The samples were microwave-irradiated (150-300 W power output) and different temperatures ranging from 150 to 170 °C were reached depending on the reaction and/or the catalyst. Reaction products were also identified and confirmed by ^{1}H NMR using a JEOL 400 spectrometer operating at 400.13 MHz. Chemical shifts were calibrated using the internal $SiMe_4$ resonance.

A typical catalytic test was performed as follows: 1 mmol benzyl alcohol, 1.2 mmol aniline, 2 mmol NaO^{t}Bu, 4 mL toluene and 0.04 catalyst were microwaved at 300 W (maximum power output) for 1 h (160-170 °C, maximum temperature reached). The final reaction mixture was analysed by GC. The response factors of the main reaction products were determined with respect to the starting materials from GC analysis using known compounds in calibration mixtures of specified compositions. Reagents were used as purchased from Sigma-Aldrich, Fluka or Avocado. Isolated yields were obtained from the resulting reaction mixture *via* filtration through celite (solvent removed under reduced pressure) and purification of the residue (if needed) by flash chromatography on silica gel (hexane–ethyl acetate) to give the corresponding products.

Catalysts were reused upon reaction finalisation. With this purpose, catalysts were filtered off after every cycle, washed with ethanol and acetone and dried overnight at 120 °C prior to their reuse in the reaction. Similar reaction conditions to those employed in each typical catalytic test (see experimental above) were employed for each reuse.

Selected examples of characterisation of isolated products, in good agreement with literature values, are given as follows:

Benzyl(phenyl)aniline[10]. Colourles oil; IR (film, cm^{-1}) ν 3420, 3069, 1606, 1512, 1323, 1240, 917; ^{1}H NMR δ 4.22 (s, 2H), 4.53 (s, ^{1}H), 6.49-6.56 (m, 2H), 6.65-6.71 (m, 1H), 7.10-7-15 (m, 2H), 7.21-7.31 (m, 5H); ^{13}C NMR δ 48.05, 112.70 (2C), 117.35, 127.05, 127.35 (2C), 128.45 (2C), 129.10 (2C), 139.30, 148.00; MS (EI) *m*/*z* 184 (M$^+$ +1, 15%), 183 (93), 182 (43), 181 (58), 180 (71), 106 (20), 104 (17), 91 (100), 78 (11), 77 (55), 65 (25), 63 (11), 51 (31).

4-Chlorobenzyl(phenyl)amine[10]. Pale yellow oil; IR (film, cm^{-1}) ν 3425, 3060, 1607, 1514, 1430, 1323, 1100;^{1}H NMR δ 3.80, 7.10-7.15 (m, 2H), 7.20-7.25 (m, 4H); ^{13}C NMR δ 47.35, 112.70 (2C), 117.57, 128.50 (2C), 128.55 (2C), 129.15 (2C), 132.60, 137.90, 147.70; MS (EI) *m*/*z* 219 (M$^+$ +2, 20%), 218 (14), 217 (73), 216 (35), 215 (47), 214 (50), 182 (10), 127 (35), 125 (100), 106 (20), 106 (10), 104 (12), 89 (23), 77 (50), 75 (11), 65 (11), 63 (12), 51 (24).

Benzyl(4-methoxyphenyl)amine[10]. Brownish oil; IR (cm^{-1}) ν 3377, 3026, 1507, 1450, 1240, 1045, 906; ^{1}H NMR δ 3.30 (s, 1H), 3.65 (s, 3H), 4.20 (s, 2H), 6.50-6.55 (m, 2H), 6.70-6.75 (m, 2H), 7.20-7.30 (m, 5H); ^{13}C NMR δ 48.95, 55.50, 114.00 (2C), 114.65 (2C), 126.75, 126.95, 127.35 (2C), 128.35 (2C), 142.25, 151.90; MS (EI) *m*/*z* 214 (M$^+$ +1, 13%), 213 (84), 212 (21), 211 (86), 210 (18), 198 (10), 197 (16), 196 (100), 169 (30), 122 (55), 92 (11), 91 (50), 77 (12), 65 (12), 63 (12).

Benzyl(4-pyridyl)amine[10]. White solid; mp 87-89 °C; IR (KBr, cm^{-1}) ν 3465, 3125, 1615, 1523, 1448, 1348, 1229;^{1}H NMR δ 4.30 (d, J = 5.6 Hz, 2H), 5.65 (s, 1H), 6.40 (d, J = 6.3 Hz, 2H), 7.20-7.35 (m, 5H), 8.05 (d, J = 5.4 Hz, 2H); ^{13}C NMR δ 46.40, 107.50, 126.95 (2C), 127.20, 128.50 (2C), 137.90, 149.30, 153.40; MS (EI) *m*/*z* 185 (M$^+$ +1, 10%), 184 (81), 183 (21), 196 (100), 91 (100), 91 (50), 78 (10), 65 (10).

Results and discussion

Materials were found to have different properties depending on the investigated support. Fe-HMS was a highly mesoporous material with high surface area (525 m^2 g^{-1}), similar to Fe-MCM-41 (>1,000 m^2 g^{-1}) and the Fe-Clay (180 m^2 g^{-1}). Fe-chitosan and Fe-cellulose, on the contrary, were non porous materials where Fe nanoparticles were supported on the surface of the biomaterials. The iron loading in all cases was found to be around 0.3-0.5 % as measured by ICP/AES (Table 1).

Fig. 1 and 2 show AC-HAADF STEM and AC-TEM images of Fe-Cellulose and Fe-HMS, respectively. AC-TEM/STEM micrographs demonstrated that iron oxide particles were generally present in the case of Fe-cellulose with an average diameter of 29.5 nm (Fig. 1). These iron oxide particles (most of them consistent with Fe_2O_3 observed by lattice imaging) consisted of 5 nm diameter averaged nanocrystals. Additionally, a small number of tiny nanoparticles (<5 nm, shown in (d) by blue arrows) were also present. Strong contrast in a) and AC-TEM lattice imaging indicated the presence of some iron single crystals in the material. Ultra small nanoclusters of iron or iron oxide clusters were not generally observed. Similar features were observed for Fe-chitosan, albeit a higher number of iron single crystals were found in this material.

In the case of Fe-HMS materials, AC-HAADF-STEM and AC-TEM studies generally indicated the presence of iron particles and iron oxide (Fig. 2a), with an increased number of

Table 1 Activity of various supported iron oxide nanoparticles [conversion (mol%) and selectivity to the amine (S_{amine}, mol%) and imine (S_{imine}, mol%)] in the *N*-alkylation of aniline with benzyl alcohol under microwave irradiation[a]

Entry	Catalyst	Fe loading (wt%)	Conversion (mol%)	S_{amine} (mol%)	S_{imine} (mol%)
1	Blank[b]	—	<5	—	—
2	Supports	—	<5	—	—
3	Fe-HMS	0.39	58	35	65
4	Fe-MCM-41	0.32	34	15	85
5	Fe-Clay	0.44	22	10	90
6	Fe-cellulose	0.29	<15	38	62
7	Fe-chitosan	0.37	40	50	50

[a] Reaction conditions: 1 mmol benzyl alcohol, 1.2 mmol aniline, 2 mmol NaO^{t}Bu, 4 mL toluene, 0.04 g catalyst, 300 W (max. power output), 1 h, 160-170 °C (max. temperature reached). [b] Without catalyst after 2 h of microwave irradiation.

iron nanocrystals compared to Fe-cellulose. The nanostructure and pores of the hexagonal mesoporous silica were also well resolved as shown in c) and d).

XPS experiments demonstrated Fe nanoparticles were essentially composed of iron oxides, mainly present as Fe^{3+} (Fe_2O_3, >60% of total Fe content) with minor quantities of Fe^0 (<5% total Fe, shoulder at ~706 eV,[16,17] Fig. 3 and 4) in the materials, regardless of the support (Fig. 3 and 4). These findings were in good agreement with results obtained by AC-(S)TEM and XRD, in which hematite (Fe_2O_3) was the predominant phase, with only minor traces of FeO found in the materials (Fig. 5). Very weak diffraction lines were found for the low loaded materials (Fig. 5, solid line), thereby needing a higher loading material (3%Fe-MCM-41) to be utilised as comparison to ascertain the Fe species in the catalysts (Fig. 5, dotted line). In any case, the supported nanoparticles possessed interesting features depending on the investigated support. Supported Fe oxides on porous materials (Fe-HMS, Fe-MCM-41 and Fe-Clay) exhibited Fe2p bands at 710-711 eV (Fe2p3/2) and 723-724 eV (Fe2p1/2), typical of the reported Fe2p binding energies of Fe_2O_3.[16]

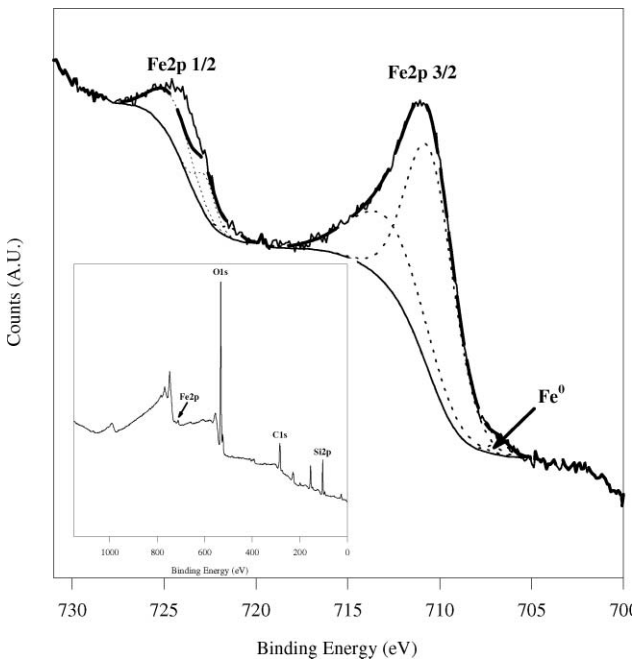

Fig. 3 XP spectra of survey (top) and Fe2p region (bottom) of Fe-HMS.

Comparatively, Fe-cellulose and Fe-chitosan materials presented Fe2p bands at remarkably lower binding energies (~708 and 721 eV, respectively, Figure 4), which may indicate a stronger interaction of the iron oxides with the support (possibly through the hydroxyl groups of the polysaccharides). These interesting observations may indicate a difference in the environment of Fe in the materials and may confer special properties and applications to these supported nanoparticles.

Having investigated the properties and nature of the supported nanoparticles on various supports, a novel microwave-assisted hydrogen autotransfer mediated *N*-alkylation process between benzyl alcohol and aniline (Scheme 1) was selected to investigate the applications of such nanomaterials in heterogeneous catalysis. Martinez *et al.* have recently shown this reaction could be carried out with high yields and selectivity to the coupling products using magnetite as catalyst.[10] Nevertheless, high quantities of catalysts and extremely long times of reaction (over 7 days) at relatively high temperatures (90 °C) were needed in order to achieve good amine yields.[10]

A preliminary screening of all catalysts in the reaction is summarised in Table 1. Initially, 1 h microwave irradiation, 300 W (maximum power output) and 0.04 g catalyst were chosen as reaction conditions. Blank runs (in the absence of catalyst)

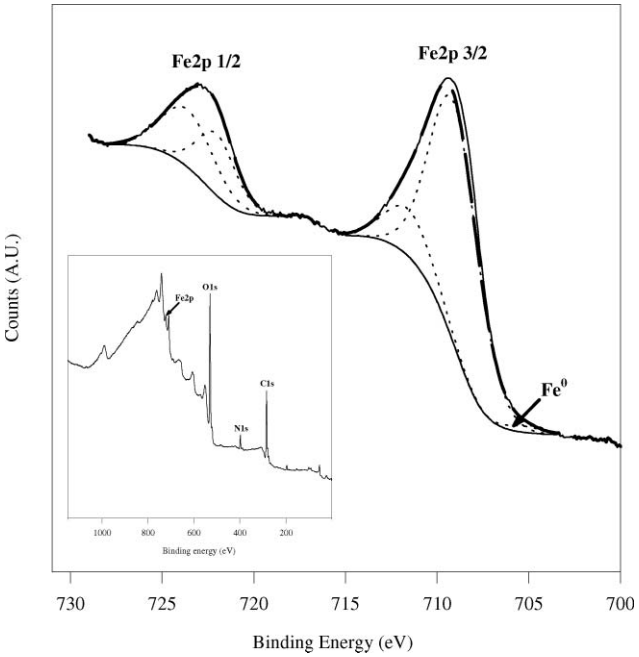

Fig. 4 XP spectra of survey (top) and Fe2p region (bottom) of Fe-chitosan.

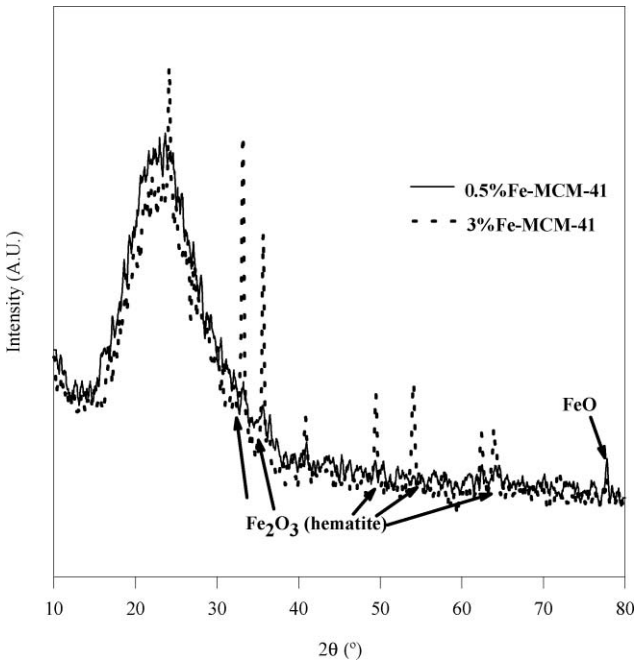

Fig. 5 XRD diffraction patterns of 0.5% and 3% Fe-MCM-41 materials.

Table 2 Effect of the time and power of microwave irradiation, quantity of catalyst, solvent and base in the activity of Fe-HMS [conversion (mol%) and selectivity to the amine (S_{amine}, mol%) and imine (S_{imine}, mol%)] in the *N*-alkylation of aniline with benzyl alcohol[a]

Investigated effect		Conversion (mol%)	S_{amine} (mol%)	S_{imine} (mol%)
Effect of microwave power	150 W	<25	15	85
	200 W	38	18	82
	250 W	50	40	60
	300 W	58	35	65
Effect of time of irradiation	0.5 h	27	25	75
	1 h	58	35	65
	1.5 h	78	60	40
	2 h	93	85	15
Effect of the quantity of catalyst	0.02 g	30	40	60
	0.04 g	58	35	65
	0.06 g	65	46	54
	0.08 g	81	67	33

[a] Reaction conditions (unless otherwise stated): 1 mmol benzyl alcohol, 1.2 mmol aniline, 2 mmol NaO^{t}Bu, 4 mL toluene, 0.04 g catalyst, 300 W (max. power output), 1 h reaction, 150-170 °C (max. temperature reached).

after 2 h of microwave irradiation gave virtually no conversion of starting material (Table 1, entry 1).

Results showed all investigated nanomaterials had moderate to low activities in the reaction with inherent low selectivities to the amine after 1 h of microwave irradiation. Of note were the activity of Fe-HMS and the interesting selectivities to the amine of Fe-cellulose and Fe-chitosan materials. We believe this peculiar selectivity for these biomaterials-supported nanoparticles might be related to the reductive properties of the supports (*via* hydroxyl groups) in Fe-cellulose and Fe-chitosan, which may facilitate the last step of hydrogen transfer to the imine (coupling intermediate) for the formation of the amine.[10]

In any case, several parameters including the time and power of microwave irradiation, the quantity of catalyst, solvent and base employed were further investigated. Results have been included in Table 2 and Fig. 6.

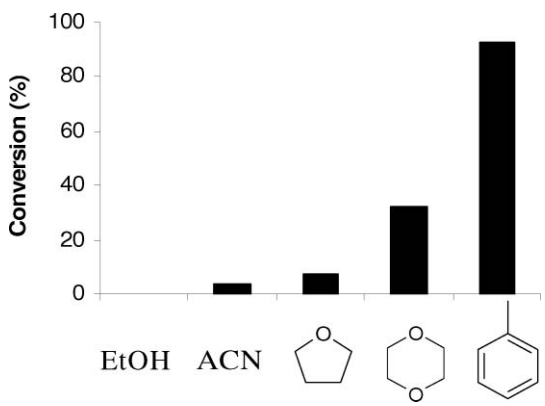

Fig. 6 Effect of the solvent in the activity of Fe-HMS in the coupling between benzyl alcohol and aniline. Reaction conditions: 1 mmol benzyl alcohol, 1.2 mmol aniline, 2 mmol NaO^{t}Bu, 4 mL solvent, 0.04 g Fe-silica, 300 W, 2 h, 160–170 °C.

An increase in both the microwave power, time of irradiation and quantity of catalyst increased, in general, both the activity and the selectivity to amine in the systems (Table 2). Under the optimum reaction conditions (2 h microwave irradiation, 300 W and 0.04 g catalyst) a 93% conversion with an 85% selectivity to the amine was obtained (Table 2). A further increase in time of irradiation and/or quantity of catalyst did not appreciably change the activity of the catalyst in the process. Comparatively, the reaction was performed under similar optimised conditions under conventional heating (under toluene reflux) to provide quantitative conversion of starting material in 24 h reaction. Interestingly, only traces of the amine were found, with the imine (Scheme 1, B) as the main reaction product under these conditions. Further runs under conventional heating showed there was no significant formation of amine under the investigated reaction conditions (including different solvents, catalysts and bases) which imply the reduction step (from imine to amine) and thus the selectivity to the amine is only favoured under microwave irradiation at short times of reaction (typically 1-2 h), in good agreement with reports proving that activities and selectivities in organic reactions can be significantly improved under microwave irradiation.[18–20]

A range of solvents were also investigated in the reaction (dioxane, THF, ethanol, acetonitrile) in order to check the effect of the solvent polarity (loss factors) in the microwave-assisted protocol. Interestingly, the best results were obtained in the least polar solvent (toluene, Fig. 6), which implies there are no relevant solvent polarity effects under microwave irradiation, probably due to the inherent polarity of the reagents (benzyl alcohol and aniline)[18] and that solubility/miscibility effects of reactants, base and catalyst in the chosen solvent are more relevant.

The base employed in the reaction also seemed to be important, especially to support the reaction mechanism. A screening of bases in the microwave-assisted protocol demonstrated Na and KO^{t}Bu were very good bases for the process, with K_2CO_3 and KOH giving very low activities in the reaction. However, the most relevant finding was obtained when DABCO was employed as a base in the reaction. We have recently reported the involvement of this nucleophilic base in metal-free Sonogashira couplings, *via* hydrogen abstraction from the alkyne.[21] Results included in Table 3 show a remarkable improvement of converted starting material (at almost equal selectivities as those found

Table 3 Activity of various supported iron oxide nanoparticles [conversion (mol%) and selectivity to the amine (S_{amine}, mol%) and imine (S_{imine}, mol%)] in the microwave-assisted selective *N*-alkylation of aniline with benzyl alcohol using DABCO as a base[a]

Entry	Catalyst	Conversion (mol%)	S_{amine} (mol%)	S_{imine} (mol%)
1	Blank (no cat.)	15	>90	<10
2	Fe-HMS	85	50	50
3	Fe-MCM-41	75	30	70
4	Fe-clay	55	20	80
5	Fe-cellulose	40	45	55
6	Fe-chitosan	70	65	35

[a] Reaction conditions: 1 mmol benzyl alcohol, 1.2 mmol aniline, 2 equiv. DABCO, 4 mL toluene, 0.04 g catalyst, 300 W (max. power output), 1 h, 160-170 °C (max. temperature reached).

Table 4 Selective *N*-alkyation of a range of amines with benzyl alcohol using Fe-HMS as catalyst under microwave irradiation[a]

Entry	Amine	Time/h	Conversion (mol%)	S_{amine} (mol%)	S_{imine} (mol%)
1		1.5	>99 (92)	90	10
2	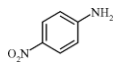	1	>99 (89)	90	10
3	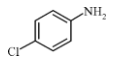	1	>99 (93)	85	15
4	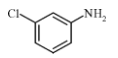	1	>95 (90)	85	15
5	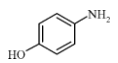	2	85 (77)	>90	<10
6	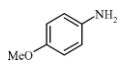	2	75	75	25
7	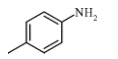	2	70	80	20
8		1.5	>99 (91)	85	15
9		1.5	>99 (93)	85	15
10		1.5	85 (78)	62	38
11		2	80	30	70
12		2	88 (86)	60	40

[a] Reaction conditions (unless otherwise stated): 1 mmol benzyl alcohol, 1.2 mmol amine, 2 equiv. DABCO, 4 mL toluene, 0.04 g Fe-HMS, 300 W (max. power output), 150-170 °C (max. temperature reached). Isolated yields (where appropriate) are given in brackets.

using NaO^{t}Bu) for Fe-silica and Fe-chitosan, respectively, when DABCO was employed as a base in the reaction.

In order to extend the scope of the protocol, a range of substituted anilines were then tested in the process under optimised conditions. Results have been summarised in Table 4. In general, the protocol was found to be amenable to a wide range of substrates and substituents and excellent conversions and selectivities to the corresponding amines were obtained in most cases (Table 4), even for the particular case of cyclic and aliphatic amines (Table 4, entries 10 to 12). Of note were the higher yields obtained for electrowithdrawing (entries 2-4) compared to electrodonating substituents (entries 5-7), in good agreement with previous findings.[10] Likewise, a range of substituted benzyl alcohols were also investigated in the process.

Results included in Table 5 show that excellent conversions and selectivities to the *N*-monoalkylated product were obtained in all cases (regardless of the substituent employed), confirming again the versatility as heterogeneous catalyst of the Fe materials.

Table 5 Selective *N*-alkylation of a range of substituted benzyl alcohols using Fe-HMS as catalyst under microwave irradiation[a]

Entry	Amine	Time/h	Conversion (mol%)	S_{amine} (mol%)	S_{imine} (mol%)
1	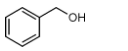	1.5	>99 (92)	90	10
2	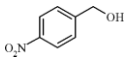	1	>99 (94)	>90	<10
3	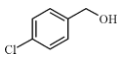	1	>99 (95)	90	10
4	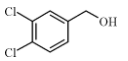	1	>99 (96)	>95	<5
5	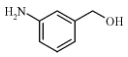	1.5	>99 (95)	88	12
6	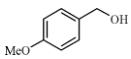	1.5	85 (77)	75	25
7	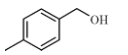	2	75	80	20
8	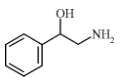	2	70	60[b]	20[b]

[a] Reaction conditions (unless otherwise stated): 1 mmol benzyl alcohol, 1.2 mmol aniline, 2 equiv. DABCO, 4 mL toluene, 0.04 g Fe-HMS, 300 W (max. power output), 150-170 °C (max. temperature reached). Isolated yields (where appropriate) are given in brackets; [b] The remaining 20% selectivity corresponds to the formation of other products.

Catalysts were also found to be highly reusable under the reaction conditions, preserving >90% of their initial activity and selectivity after 3 reuses. No Fe leaching was detected in the final reaction mixture upon recycling of the catalyst (measured by ICP/AES).

The reaction mechanism of these so-called hydrogen autotransfer processes has been well established for C–C bond forming processes.[1,2,4] It involves a domino reaction which starts with an initial hydride abstraction from one of the reagents, followed by different types of reactions between the two reagents, and completed with a reductive hydrogen addition to give the final product, a redox 2-step sequence in which the supported Fe oxides seem to play a key role (Scheme 2).[1,4,10]

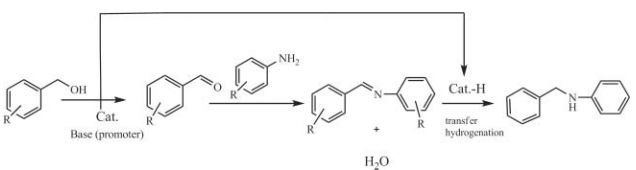

Scheme 2 General mechanism for the *N*-akylation of substituted anilines with benzyl alcohols as electrophiles *via* hydrogen autotransfer processes.

Firstly, the reactions do not work in the absence of base (sodium *tert*-butoxide or DABCO), which implies the catalytic cycle may start with the deprotonation/dehydrogenation of the alcohol promoted by the base and subsequently catalysed by the supported iron oxide nanoparticles. The evidences for this claim

are supported by the fact that only traces of products (up to 15 % conversion with DABCO, Table 3, entry 1) were obtained in the absence of catalyst after 2 h (Table 1) but the addition of catalyst drives the reaction to the production of the selective *N*-alkylated products. In this step, we believe iron oxides might be partially reduced to form Fe hydride species, in agreement with previous reports.[1,2,4,10]

Furthermore, the base was also found to play a critical role in terms of reaction rates (selectivity was almost unaffected by the addition of different bases). In this way, the addition of DABCO, a nucleophilic base highly effective in metal-free catalysed couplings,[21] provided improved yields at shorter times of reaction, confirming the involvement of alcohol deprotonation as a first reaction step (alcohol as electrophile, Scheme 2).

In the second step, an S_N2 displacement reaction takes place and leads to the formation of the imine compounds that are subsequently reduced by the Fe hydride species to give the observed *N*-alkylated products. This reduction step has been proved to be a transfer hydrogenation reaction that was actually promoted only under microwave irradiation when a base (*e.g.* sodium *tert*-butoxide) as well as a proper hydrogen donor (2-propanol, 1 mL added to the mixture) were present in solution, in good agreement with previous reports on hydrogen transfer metal catalysed reactions.[22] Interestingly, the high selectivities observed for the Fe-chitosan catalyst might well be related to the reductive capacity of the hydroxyl groups in the polysaccharide backbone, sufficient to reduce metal cations in solution to supported nanoparticles,[11,23] a fact that will also correlate well with the strong interaction Fe-support observed in the XPS of these materials (Fig. 4).

Conclusions

We have reported the preparation of versatile Fe oxide nanoparticles supported on a variety of (bio)materials that are catalytically active in the selective *N*-alkyation of (substituted) amines with benzyl alcohols. Fe-HMS was found to be the most active catalyst in the reaction with Fe-chitosan showing the best amine selectivities. We envisage these materials to be applicable in other couplings as well as many different redox catalysed processes that are currently under investigation in our laboratories.

Acknowledgements

CG-A is grateful to Ministerio de Educación y Ciencia and Fundación Española para la Ciencia y Tecnología for a funded fellowship and RL to Ministerio de Ciencia e Innovación for a Ramon y Cajal contract (RYC-2009-04199). The authors also thank the University of York, Yorkshire Forward/EU and JEOL, for sponsoring the York JEOL Nanocentre and KY thanks the Japan Society for Promotion of Science/Japan Fine Ceramic Center (JSPS/JFCC) for a fellowship.

Notes and references

1 G. Guillena, D. J. Ramon and M. Yus, *Chem. Rev.*, 2010, **110**, 1611.
2 (*a*) A. Baiker and J. Kijenski, *Catal. Rev. Sci. Eng.*, 1985, **27**, 653–697; (*b*) D. M. Roundhill, *Chem. Rev.*, 1992, **92**, 1–27.
3 (*a*) R. R. Egan, *J. Am. Oil Chem. Soc.*, 1968, **45**, 481–486; (*b*) S. Arif, *Surfactant Science Series: Detergency of special surfactants*, Ed. F. Friedli, Marcel Dekker, New York, 2001, 98, 71-115; (*c*) K. S. Hayes, *Appl. Catal., A*, 2001, **221**, 187–195; (*d*) H. A. Wittcoff, B. G. Reuben and J. S. Plotkin, *Industrial Organic Chemicals*, Wiley-Interscience, Hoboken, New Jersey, 2004.
4 G. Guillena, D. J. Ramon and M. Yus, *Angew. Chem., Int. Ed.*, 2007, **46**, 2358–2364.
5 (*a*) Y. Horikawa, Y. Uchino and T. Sato, *Chem. Lett.*, 2003, **32**, 232–233; (*b*) Y. Sprinzak, *J. Am. Chem. Soc.*, 1956, **78**, 3207–3208.
6 (*a*) S. Narayanan and B. P. Prasad, *J. Chem. Soc., Chem. Commun.*, 1992, 1204–1205; (*b*) F. Valot, F. Fache, R. Jacquot, M. Spagnol and M. Lemaire, *Tetrahedron Lett.*, 1999, **40**, 3689–3692.
7 (*a*) F. Alonso, P. Riente and M. Yus, *Eur. J. Org. Chem.*, 2008, 4908–4914; (*b*) J. L. Garcia-Ruano, A. Parra, J. Aleman, F. Yuste and V. M. Mastranzo, *Chem. Commun.*, 2009, 404–406.
8 (*a*) A. Baiker and W. Richarz, *Synth. Commun.*, 1978, **8**, 27–32; (*b*) T. Yamakawa, I. Tsuchiya, D. Mitsuzuka and T. Ogawa, *Catal. Commun.*, 2004, **5**, 291–295; (*c*) H. Kimura and H. Taniguchi, *Appl. Catal., A*, 2005, **287**, 191–196.
9 B. Ohtani, H. Osaki, S. I. Nishimoto and T. Kagiya, *J. Am. Chem. Soc.*, 1986, **108**, 308–310.
10 R. Martinez, D. J. Ramon and M. Yus, *Org. Biomol. Chem.*, 2009, **7**, 2176–2181.
11 C. Gonzalez-Arellano, J. M. Campelo, D. J. Macquarrie, J. M. Marinas, A. A. Romero and R. Luque, *ChemSusChem*, 2008, **1**, 746–750.
12 C. Gonzalez-Arellano, R. Luque and D. J. Macquarrie, *Chem. Commun.*, 2009, 1410–1412.
13 R. Luque, J. M. Campelo, D. Luna, J. M. Marinas and A. A. Romero, *Microporous Mesoporous Mater.*, 2005, **84**, 11–20.
14 D. J. Macquarrie, B. C. Gilbert, L. J. Gilbey, A. Caragheorgheopol, F. Savonea, D. B. Jackson, B. Onida, E. Garrone and R. Luque, *J. Mater. Chem.*, 2005, **15**, 3946–3951.
15 S. J. Pennycook and L. A. Boatner, *Nature*, 1988, **336**, 565–567.
16 C. D. Wagner, W. N. Riggs, L. E. Davis, G. F. Moulder and G. E. Muilenberg, (ed.), (*Handbook of X-Ray Photoelectron Spectroscopy*, Perkin Elmer, Eden Praine, 1979.
17 C. Carja, Y. Kameshima and K. Okada, *Microporous Mesoporous Mater.*, 2008, **115**, 541–547and referencestherein .
18 C. O. Kappe, *Angew. Chem., Int. Ed.*, 2004, **43**, 6250–6284.
19 V. Polshettiwar and R. S. Varma, *Chem. Soc. Rev.*, 2008, **37**, 1546–1557.
20 V. Polshettiwar and R. S. Varma, *Acc. Chem. Res.*, 2008, **41**, 629–639.
21 R. Luque and D. J. Macquarrie, *Org. Biomol. Chem.*, 2009, **7**, 1627–1632.
22 M. J. Gracia, J. M. Campelo, E. Losada, R. Luque, J. M. Marinas and A. A. Romero, *Org. Biomol. Chem.*, 2009, **7**, 4821–4824.
23 P. Mukherjee, C. R. Patra, A. Ghosh, R. Kumar and M. Sastry, *Chem. Mater.*, 2002, **14**, 1678–1684.